Influence of shear flows on dynamic evolutions of double tearing modes

W. Zhang[1], Z. W. Ma[1,*], X. Q. Lu[2,*], and H. W. Zhang[1]

[1]Institute for Fusion Theory and Simulation, Department of Physics, Zhejiang University, Hangzhou 310027, China

[2]College of Nuclear Equipment and Nuclear Engineering, Yantai University, Yantai 264005, China

Abstract: Influences of shear flows on dynamic evolutions of the *m*/*n*=2/1 double tearing mode (DTM) are investigated using the three-dimensional, toroidal, and nonlinear resistive magnetohydrodynamic code CLT. It is found that weak shear flows can lead to the decoupling of tearing modes on the two resonant surfaces and reduce the linear growth rate of DTMs. When the two tearing modes grow up to a large amplitude at the nonlinear stage, they start to lock with each other. Consequently, DTMs with weak shear flows exhibit almost the same behavior as that without shear flows, i. e. the weak shear flow almost has no influence on the time and the amplitude of the pressure crash. It is also found that the linear growth rates of the modes can become even larger than that without shear flows when the shear flow exceeds a critical value due to the Kelvin-Helmholtz (KH)-like instability. The KH-like instability can broaden the spectrum of the modes and then form a broad region with stochastic magnetic fields. Therefore, strong shear flows might be even more destructive for the plasma confinement.

[a)] Corresponding Author: zwma@zju.edu.cn and luxingqiang@163.com

I. Introduction

In tokamaks, the reversed magnetic shear in the central region is crucial for forming the internal transport barrier, increasing the plasma beta, and significantly improving the energy confinement.[1-3] Therefore, the reversed magnetic shear configuration is recognized as one of the advanced scenarios in tokamak operations.[4-6] However, such a system is subject to the double tearing modes (DTMs) since there exist two resonant surfaces with the same helicity. The linear growth rate of DTMs is $\gamma \sim S^{-1/3}$, which is much faster than the single tearing mode ($\gamma \sim S^{-3/5}$), where S is the Lundquist number. Besides, the nonlinear evolution of DTMs could lead to a significant reduction of the plasma pressure and degradation of the energy confinement during tokamak discharge.[7-9] Hence, it is necessary to understand the mechanism of DTMs, and develop effective methods to suppress DTMs.[10-27]

The large growth rates of DTMs mainly result from the coupling between the two tearing modes on the neighboring resonant surfaces. One can expect that DTMs will develop much slower if the two tearing modes are decoupled. The methods to decouple DTMs are shear flows [14, 26, 28-30], diamagnetic effects [31], or modifications of the current profile by external current drive.[17, 32] As the neutral beam injection (NBI) can not only help to form a reversed shear configuration but also lead to strong shear flows [33-35], we should always consider influences of shear flows when studying dynamic evolution of DTMs.

If the shear flow is weak, it leads to decoupling the tearing modes on the two resonant surfaces and then reducing the linear growth rate of DTMs from $S^{-1/3}$ to $S^{-3/5}$. When the shear flow is strong, the system can be unstable for the Kelvin-Helmholtz (KH)-like instability.[36, 37] However, it is still not clear whether shear flows could prevent the violent pressure crash. Therefore, in the present paper, we carry out a systematical study of DTM by using the three-dimensional, toroidal,

magnetohydrodynamic (MHD) code CLT. It is found that weak shear flows could decouple DTMs and then decrease their linear growth rates. However, due to the mode-locking effect, the two tearing modes can lock with each other at the nonlinear stage. After the modes become locked, the DTM with shear flows exhibits almost the same behavior as that without shear flows, i. e. the time and the amplitude of the pressure crash are nearly unaffected by the shear flow. It indicates that the weak shear flow only reduces the linear growth rate of the DTM, but it cannot prevent the violent pressure crash. If the shear flow exceeds a critical value, the linear growth rate of the DTM is even larger than that without shear flows. Although the two tearing modes cannot lock with each other, the strong shear flow can lead to the KH-like instability[36, 37] at the nonlinear stage, which drives instabilities with other helicities and form a vast region with the stochastic magnetic field. The spectrum of modes is broad, and the poloidal mode number of dominant modes is $m \sim 11$. It is found that the plasma viscosity becomes important when the shear flow reaches a critical value. With a sufficiently high viscosity, the magnetic islands can easily lock with each other at the nonlinear stage and vice versa.

II. Numerical Model

The compressible resistive MHD equations used in CLT[38] are given as follows:

$$\frac{\partial \rho}{\partial t} = -\nabla \cdot (\rho \mathbf{v}) + \nabla \cdot [D \nabla (\rho)], \tag{1}$$

$$\frac{\partial p}{\partial t} = -\mathbf{v} \cdot \nabla p - \Gamma p \nabla \cdot \mathbf{v} + \nabla \cdot (\kappa_{\perp} \nabla p) + \nabla_{\parallel} \cdot (\kappa_{\parallel} \nabla_{\parallel} p), \tag{2}$$

$$\frac{\partial \mathbf{v}}{\partial t} = -\mathbf{v} \cdot \nabla \mathbf{v} + (\mathbf{J} \times \mathbf{B} - \nabla p) / \rho + \nabla \cdot (\nu \nabla \mathbf{v}), \tag{3}$$

$$\frac{\partial \mathbf{B}}{\partial t} = -\nabla \times \mathbf{E}, \tag{4}$$

$$\mathbf{E} = -\mathbf{v} \times \mathbf{B} + \eta \mathbf{J}, \tag{5}$$

$$\mathbf{J} = \nabla \times \mathbf{B}, \tag{6}$$

Where ρ, p, $\mathbf{v}$, $\mathbf{B}$, $\mathbf{E}$, and $\mathbf{J}$ are the plasma density, the plasma pressure, the fluid velocity, the magnetic field, the electric field and the current density, respectively. It should be noted that, instead of the classical 8-field MHD equations, we choose to use $\mathbf{E}$ as an intermediate value to solve the Faraday's law. This method is helpful to keep $\nabla\bullet\mathbf{B}=0$ during the simulation. Γ is the ratio of specific heat of the plasma. All the variables are normalized as follows: $\mathbf{x}/a\rightarrow\mathbf{x}$, $t/t_A\rightarrow t$, $\rho/\rho_{00}\rightarrow\rho$, $p/(B_0^2/\mu_0)\rightarrow p$, $\mathbf{v}/v_A\rightarrow\mathbf{v}$, $\mathbf{B}/B_0\rightarrow\mathbf{B}$, $\mathbf{E}/(v_AB_0)\rightarrow\mathbf{E}$, and $\mathbf{J}/(B_0/\mu_0 a)\rightarrow\mathbf{J}$, where B_0, ρ_{00} and a are the initial magnetic field, the plasma density at the magnetic axis, and the minor radius, respectively. $v_A=B_0/\sqrt{\mu_0\rho_{00}}$ is the Alfvén speed, and $t_A=a/v_A$ is the Alfvén time. η, D, $\kappa_\perp$, $\kappa_\parallel$, and ν are the resistivity, the plasma diffusion coefficient, the perpendicular, and parallel thermal conductivity, and the viscosity, respectively. These parameters are normalized as follows: $\eta/(\mu_0 a^2/t_A)\rightarrow\eta$, $D/(a^2/t_A)\rightarrow D$, $\kappa_\perp/(a^2/t_A)\rightarrow\kappa_\perp$, $\kappa_\parallel/(a^2/t_A)\rightarrow\kappa_\parallel$, and $\nu/(a^2/t_A)\rightarrow\nu$, respectively.

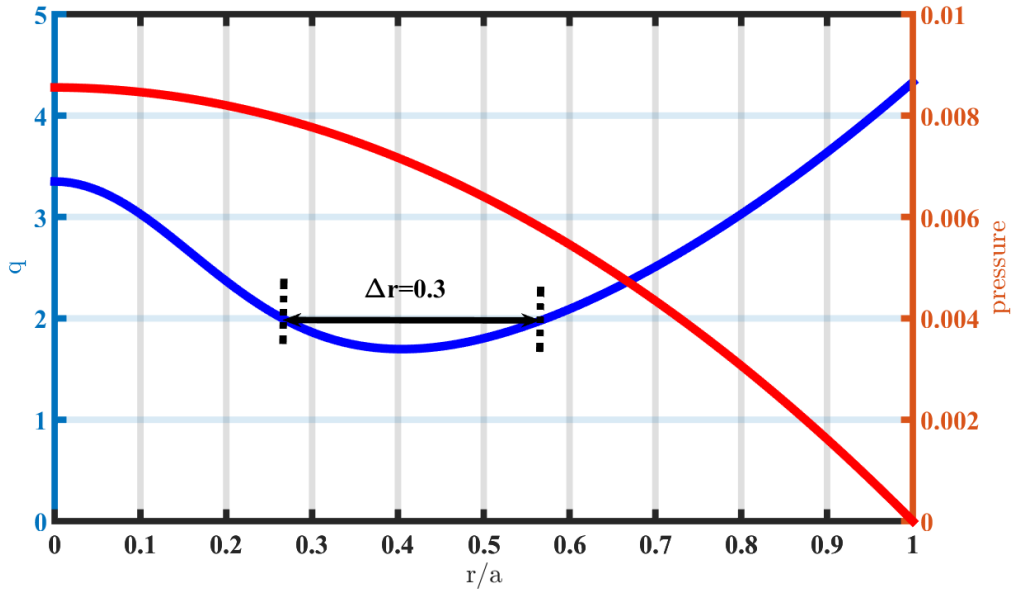

Figure 1 Initial safety factor profile and pressure profile. The distance between the

two resonant surfaces with q=2 is $\Delta r = 0.3$.

III. Simulation results

In the present paper, the parameters of TFTR[1, 7] are used, i. e., the major radius $R_0 = 2.60m$, the minor radius ($a = 0.94m$) for a circular cross-section geometry, the toroidal field $B_0 \sim 4.2T$, the electron density $n_e \sim 1.0\times10^{20}m^3$. The normalized parameters are chosen to be $\eta = 1.0\times10^{-6}$, $\nu = 1\times10^{-5}$, $\kappa_\perp = 5\times10^{-6}$, $\kappa_\parallel = 5\times10^{-2}$ and $D = 1\times10^{-4}$. The grids used in the present paper are $256\times32\times256\,(R,\varphi,Z)$. The convergence of the code has been ensured by varying both the resolutions of time and space. The initial safety factor and pressure profiles are shown in Figure 1. The distance between two resonant surfaces with q=2 is $\Delta r = 0.3$. With these parameters, the DTM causes the core-crash sawtooth that significantly reduces the plasma pressure in the core region. The initial toroidal angular velocity Ω is assumed to be

$$\Omega = 0.5*\Omega_0[1-\tanh(\frac{\bar{\psi}-\psi_0}{\Delta\psi})], \tag{7}$$

where Ω_0 is the toroidal angular velocity at the magnetic axis, $\bar{\psi}$ is the normalized poloidal magnetic flux, $\psi_0 = 0.1759$ is where the maximum flow shear is located, and $\Delta\psi = 0.0761$ is the width of the flow shear, respectively. The profiles of the shear flow with $\Omega_0 = 0.006$ is shown in Figure 2. The angular velocity at the inner and outer rational surfaces are $\Omega_1 = 0.0056$ and $\Omega_2 = 0.0001$. The difference is $\Delta\Omega = \mid \Omega_1 - \Omega_2 \mid = 0.0055$. Different from many previous studies, the shear flow here is self-consistently included in the equilibrium. As we discussed in our previous paper[39], the Tokamak equilibrium with toroidal flows could be solved through the QSOLVER code [40].

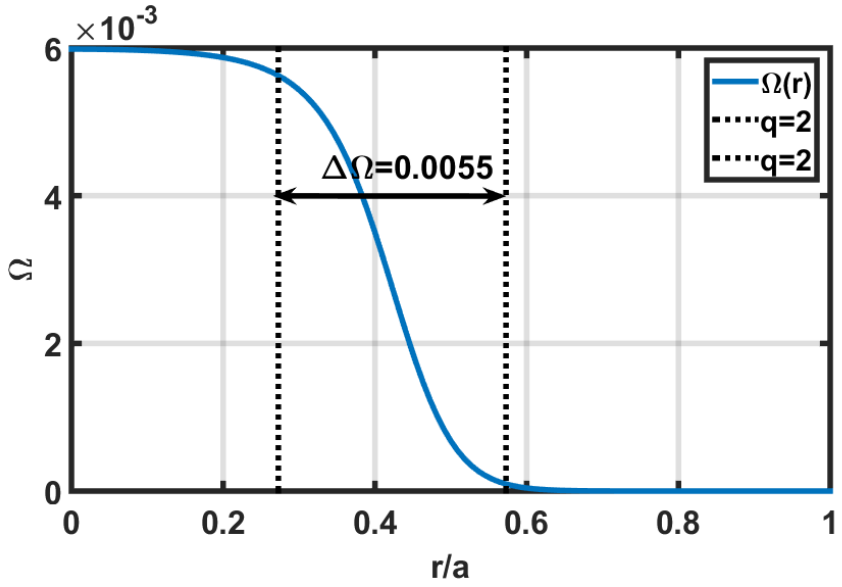

Figure 2 The profiles of the shear flow with $\Omega_0 = 0.006$. The difference of the rotation frequency between the two q=2 resonant surfaces is $\Delta\Omega = 0.0055$.

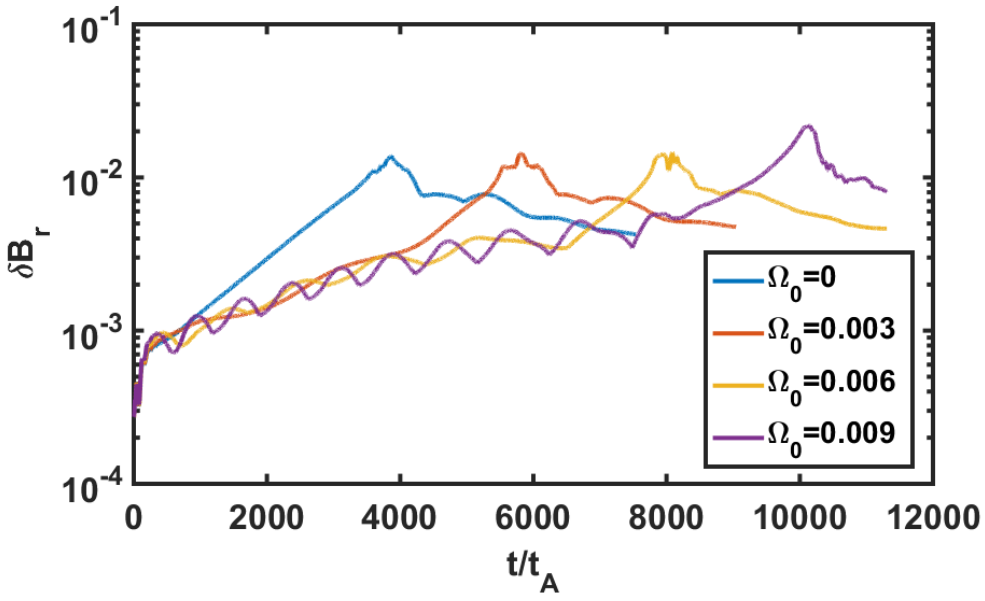

Figure 3 Evolutions of the radial perturbed magnetic field δB_r with different toroidal angular velocities $\Omega_0 = 0$, $\Omega_0 = 0.003$, $\Omega_0 = 0.006$, and $\Omega_0 = 0.009$.

A. Influence of weak shear flows

Since the width of the magnetic island can be estimated by $w \sim (\delta B_r)^{1/2}$ for

tearing modes ($m \geq 2$), δB_r is used to reflect the development of the DTM. The evolutions of the radial perturbed magnetic field δB_r with different toroidal angular velocity $\Omega_0 = 0$, $\Omega_0 = 0.003$, $\Omega_0 = 0.006$, and $\Omega_0 = 0.009$ are shown in Figure 3. The two tearing modes always couple with each other and keep anti-phase without shear flows. While, with shear flows, the tearing modes are decoupled when their amplitudes are small. Due to the decoupling of the tearing modes, the two tearing modes become periodically in-phase and anti-phase during the linear growth, and the tearing modes experience the suppression and stimulation phases periodically, which leads to that the oscillation of the amplitudes of the DTMs. Therefore, the average growth rate decreases with increasing Ω_0 when $\Omega_0 \leq 0.009$, which is consistent with many previous studies.[14, 30]

However, as shown in Figure 3, the amplitudes of the tearing modes stop oscillating when they enter into the nonlinear stage. The nonlinear evolutions of the modes are quite similar for the cases with or without the shear flow. It indicates that the decoupled modes gradually become coupled as they evolve into the nonlinear stage. The two tearing modes finally become fully coupled and locked each other when their amplitudes exceed the critical value. The Poincare plots for the case with $\Omega_0 = 0.006$ at (a) t=2185.9, (b) t=2487.4, (c) t=2864.3, (d) t=3391.9, (e) t=6783.8, (f) t=7160.7, (g) t=7537.6, and (h) t=7914.5 are shown in Figure 4. With the shear flow, the magnetic islands on the inner resonant surface rotate much faster than the islands on the outer resonant surface. Figure 4a-4d present one cycle of the poloidal rotation of the inner islands, during which the two tearing modes evolve from anti-phase to in-phase (Figure 4a~4c), then to anti-phase (Figure 4d) at t=3391.9. When the magnetic islands are large enough, the two tearing modes strongly couple and become locked with each other. Then the phase difference ($\Delta\phi$) between the two tearing modes remains $\Delta\phi = \pi$ until the core pressure crash occurs. The evolutions of the phases of the two tearing modes (ϕ_{in} and ϕ_{out}) and the phase difference between them are shown in Figure 5. Figure 5 also indicates the decoupling of the tearing modes at the linear stage and the mode-locking at the nonlinear stage. The phase difference between the two tearing modes is $\Delta\phi = \pi$ when the modes are locked with each other.

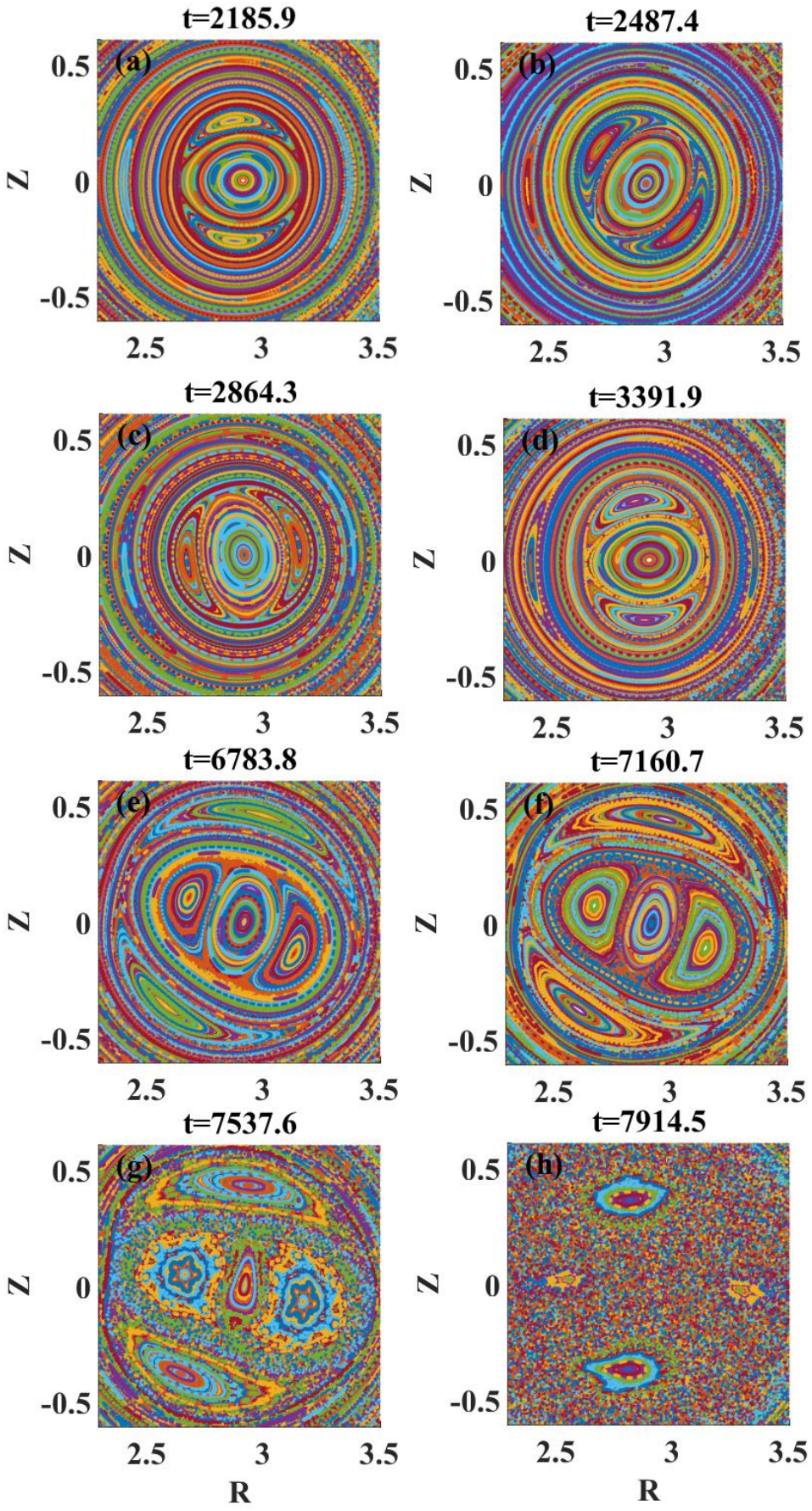

Figure 4 The Poincare plots for the case with $\Omega_0 = 0.006$ at (a) t=2185.9, (b)

t=2487.4, (c) t=2864.3, (d) t=3391.9, (e) t=6783.8, (f) t=7160.7, (g) t=7537.6, and (h) t=7914.5. (a)~(d) are a cycle, during which the magnetic islands on the two resonant surfaces are from anti-phase to in-phase and then to anti-phase. (e)-(f) clearly show that the 'mode-locking' occurs at the nonlinear stage of the DTM.

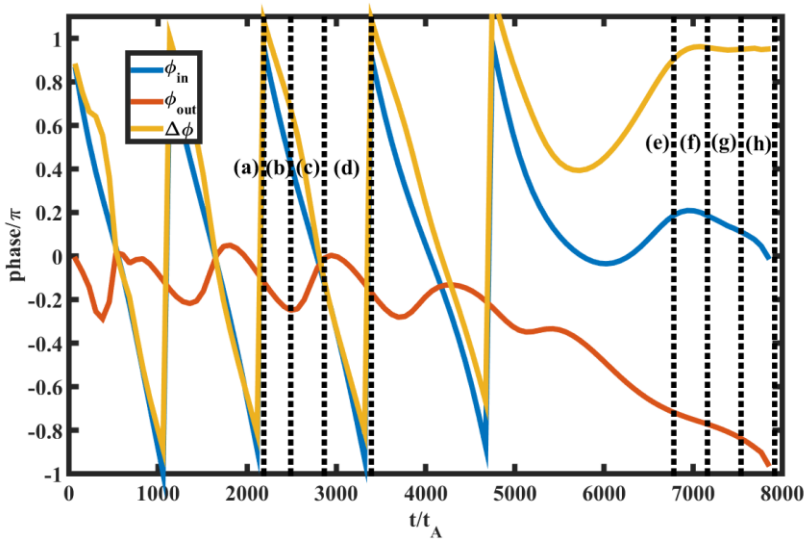

Figure 5 The evolutions of the phases of the two tearing modes (ϕ_{in} and ϕ_{out}) and the phase difference ($\Delta\phi = \phi_{in} - \phi_{out}$) between them. The moments in Figure 4 are also indicated by vertical dashed lines.

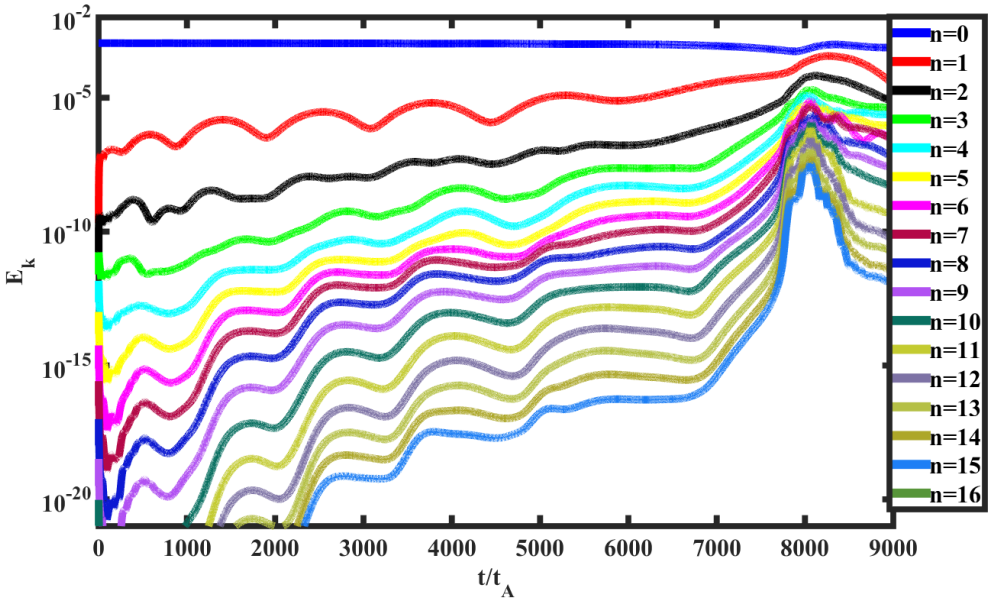

Figure 6 Kinetic energy evolutions of different toroidal modes for the case with

$\Omega_0 = 0.006$.

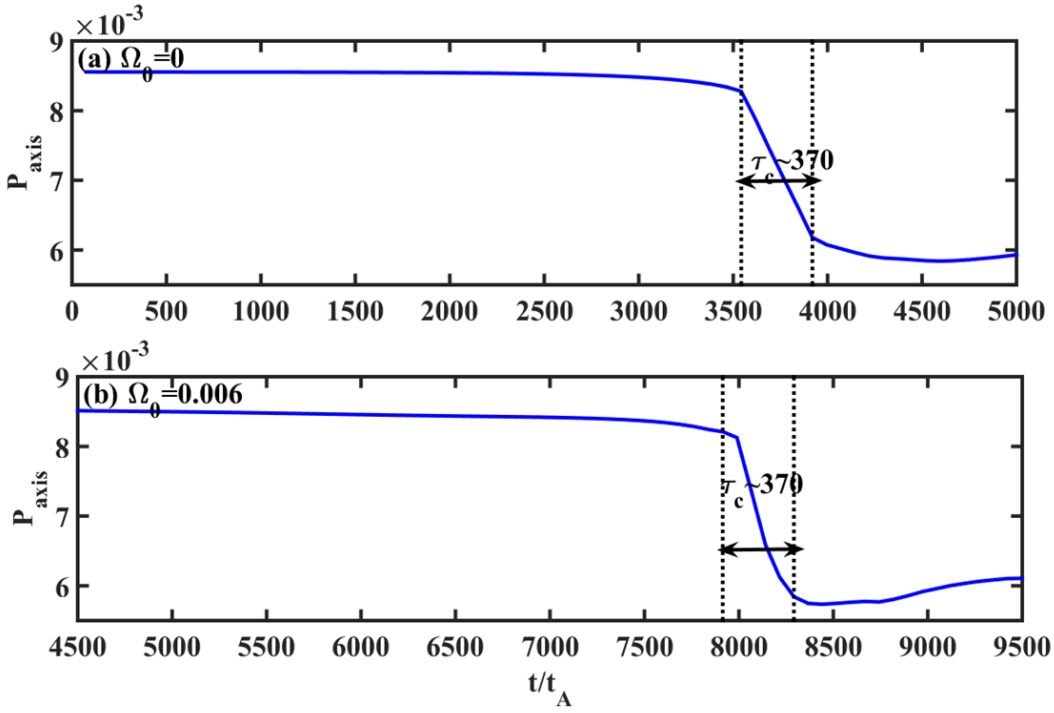

Figure 7 Evolutions of the plasma pressure at the magnetic axis for (a) $\Omega_0 = 0$ and (b) $\Omega_0 = 0.006$.

The time evolutions of the kinetic energy of different toroidal modes with $\Omega_0 = 0.006$ are shown in Figure 6. It should be noted that, after the modes are locked, the behavior of the kinetic energy becomes almost the same as that without shear flows (the details could be seen from Ref. [41]), i. e. they both experience explosive growth before the pressure crash happens. It is because the two tearing modes strongly couple with each other when their amplitudes are sufficiently large and can overcome the decoupling effect of the shear flow. Thereafter, the dynamic evolutions of the DTM with or without shear flows are similar. As we know, the nonlinear evolution of the DTM can cause a violent pressure crash in the core region (i.e., the core-crash sawtooth[7]). The shear flow is supposed to be an effective method to suppress the DTM and control this kind of fast pressure crash. However, as shown in

Figure 7, the time scales of the pressure crashes are almost the same ($\tau_c \sim 370 t_A$), and the on-axis plasma pressures are both reduced by 30% of their initial values. The profiles of the plasma pressure in the case with $\Omega_0 = 0.006$ (a) just before the pressure crash and (b) after the pressure are shown in Figure 8. Very similar to the case without shear flows, the hot region becomes narrow and elongated before the pressure crash, then a violent pressure crash occurs, and the pressure profiles become flattened in the core region. It indicates that the pressure crash at the magnetic axis is almost unaffected by the shear flow. In other words, the shear flow only affects the linear growth time of the tearing modes for the core crash sawtooth. When the tearing modes lock with each other, the nonlinear behavior of the DTM with shear flows will become almost the same as that without shear flows.

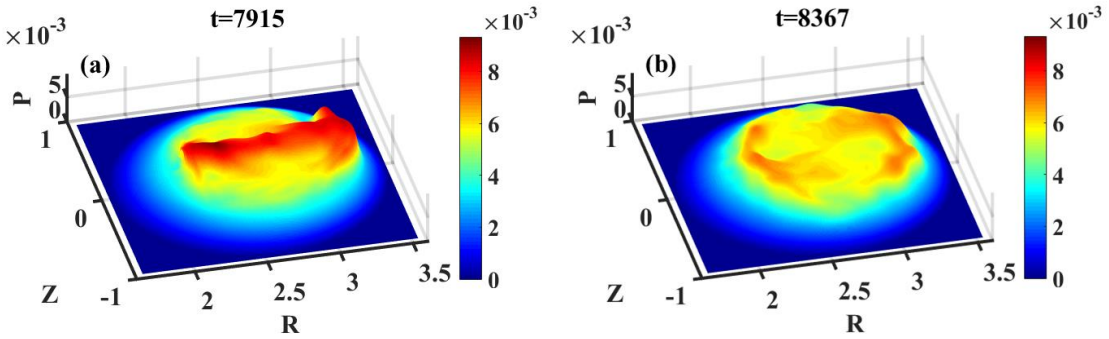

Figure 8 The pressure profiles (a) just before the pressure crash and (b) after the pressure crash.

B. Influence of strong shear flows

In some experiments with unbalanced high-power NBI,[35] the shear flow can be as large as the sound speed ($c_s = v_A \sqrt{\Gamma \beta / 2}$, which is about $0.1 v_A$ in the present paper). In the case in Section III. A, the shear flow is only $v_0 \sim 0.03 v_A$, which is much lower than c_s. In this section, we will show the dynamic evolution of the DTM with strong shear flows.

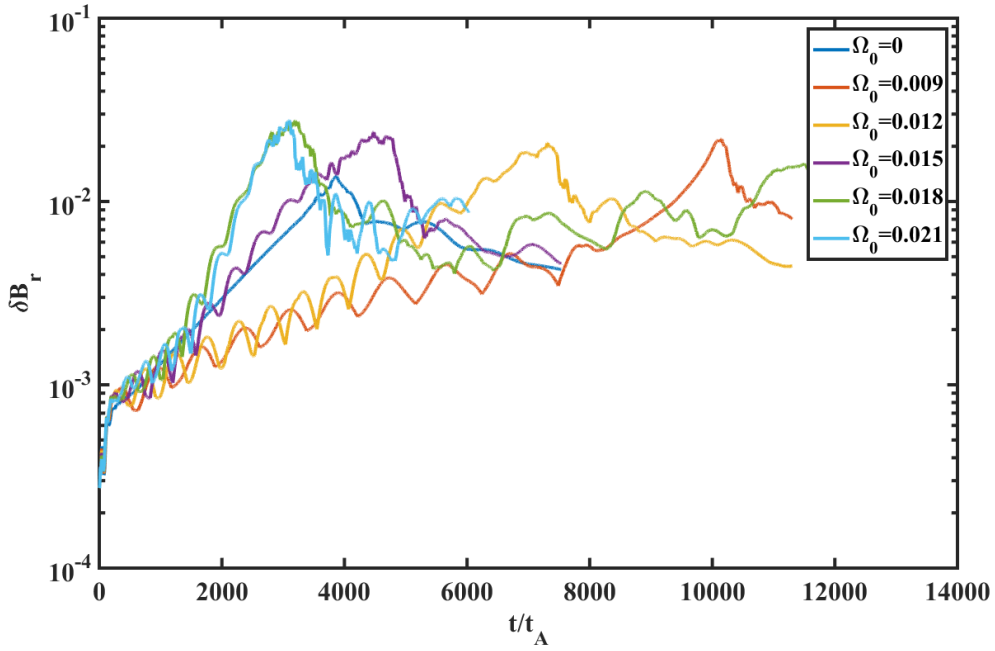

Figure 9 Evolutions of the radial perturbed magnetic field δB_r with different toroidal angular velocities $\Omega_0 = 0$, $\Omega_0 = 0.009$, $\Omega_0 = 0.012$, $\Omega_0 = 0.015$, $\Omega_0 = 0.018$, and $\Omega_0 = 0.021$.

The evolutions of the perturbed radial magnetic perturbations with different toroidal angular velocities $\Omega_0 = 0$, $\Omega_0 = 0.009$, $\Omega_0 = 0.012$, $\Omega_0 = 0.015$, $\Omega_0 = 0.018$ and $\Omega_0 = 0.021$ are shown in Figure 9. It is found that the growth rate increases with increasing Ω_0 due to the K-H like instability when $\Omega_0 > 0.009$.[30, 36] Different from that with weak shear flows, the two tearing modes with strong shear flows cannot be locked with each other even the magnetic islands are large. The DTMs still experience accelerating development at the nonlinear stage. However, the acceleration here is different from that in Figure 3, which is resulted from mode-locking between the tearing modes on the two resonant surfaces.

The two tearing modes are unable to be locked with each other in these cases. Instead, the islands on the two resonant surfaces collide when the magnetic islands on two resonant surfaces grow up to sufficient large (i.e., $w_1 + w_2 > \Delta r$, where w_1, w_2, and Δr are the width of the inner and outer islands, and the separation of two

resonant surfaces, respectively.), which can be seen from the Poincare plots of the magnetic field with $\Omega_0 = 0.018$ as shown in Figure 10. As we can see, the boundaries of the islands become unclear after the islands collide. Magnetic field lines begin to become stochastic due to overlap between the islands. As the mode further grows up, the stochastic magnetic field expands and eventually occupies the whole central region, except for the vicinity of the magnetic axis.

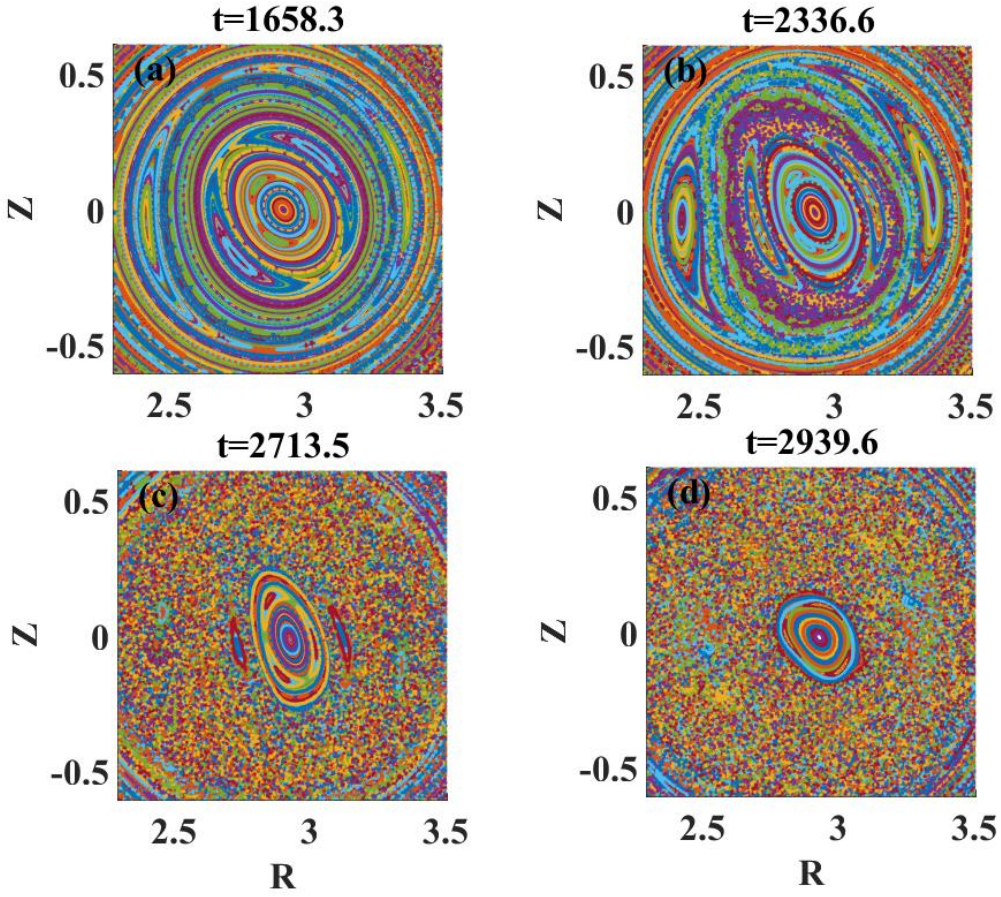

Figure 10 The Poincare plots of the magnetic field with $\Omega_0 = 0.018$. The stochasticity also can also be reflected by the Fourier analysis of the mode structures. As shown in Figure 11, all the modes with different helicities are well developed and expanded into a broad region with $\Omega_0 = 0.018$ (Figure 11a) while all the modes are basically located at their resonant surfaces without shear flows (Figure 11b). The energy spectrums at the same time with Figure 11 are shown in Figure 12. Although the amplitude of the mode *m/n*=2/1 is still the largest one, other higher helicity modes grow up to considerable amplitudes, which is significantly different from that without

shear flows. The broad energy spectrum and the dominant poloidal mode number around $m \sim 11$ are suggested to be associated with the KH-like instabilities. [36, 37] With many different helicities in the same region, the flux surfaces are destroyed, and the magnetic field becomes stochastic.

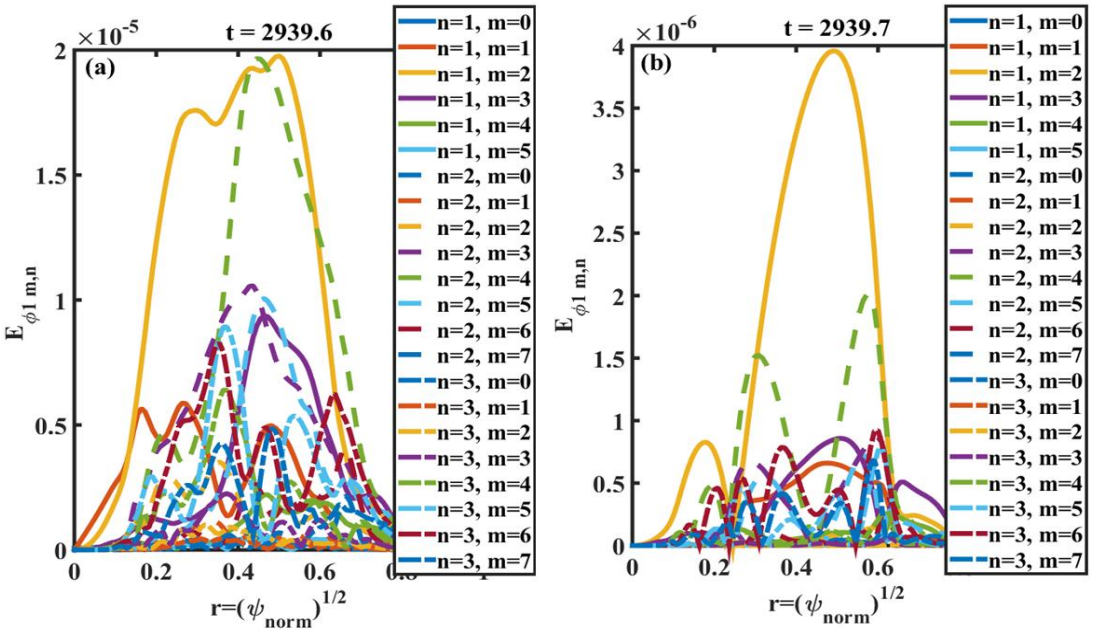

Figure 11 The mode structures (a) $\Omega_0 = 0.018$ and (b) $\Omega_0 = 0$ at $t = 2940 t_A$.

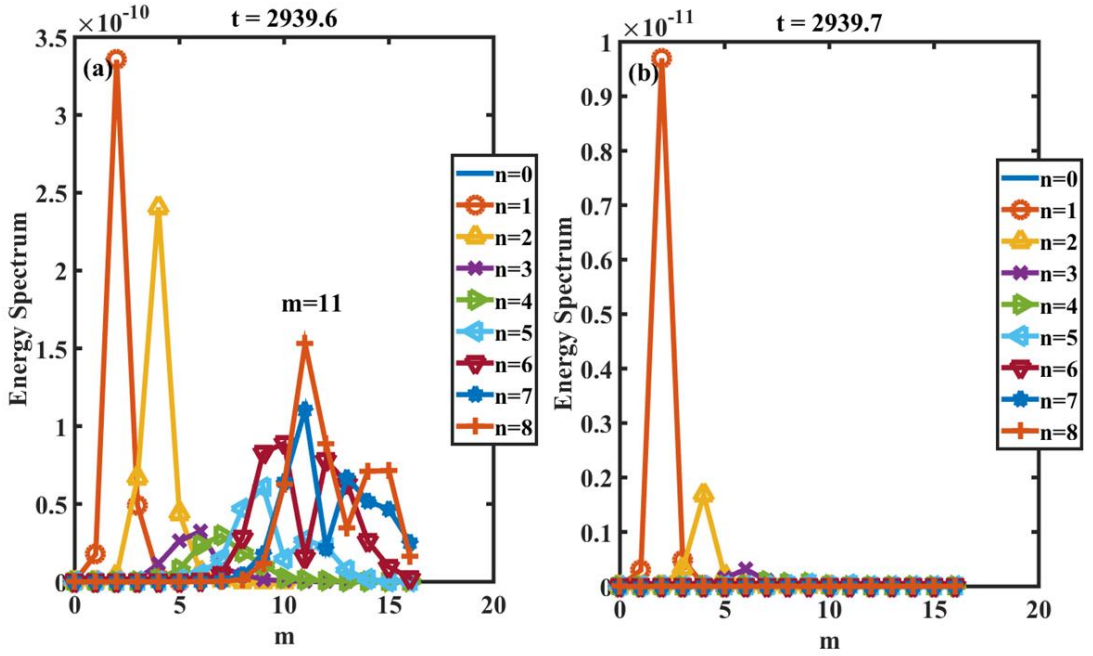

Figure 12 Energy spectrums (a) $\Omega_0 = 0.018$ and (b) $\Omega_0 = 0$ at $t \sim 2940 t_A$.

C. Influence of viscosities

As shown in the above subsection, the transition condition between the mode-locking and the stochastic magnetic field is about $\Omega_0 = 0.009$. Since the plasma viscosity could strongly influence the KH instability, we conduct systematic simulations to investigate the influence of the viscosity on the nonlinear evolution of the DTM with shear flows (Figure 13). With $\Omega_0 \le 0.009$, the two tearing modes on the two resonant surfaces can be locked with each other at the nonlinear stage. With $\Omega_0 > 0.012$, the magnetic islands on the two resonant surfaces collapses due to the collision, and the magnetic field in a broad region becomes stochastic. However, with $\Omega_0 = 0.012$, the nonlinear evolutions of the DTM with different viscosity are significantly different. The modes become locked with each other for $\upsilon = 3\times10^{-5}$; for $\upsilon \le 1\times10^{-5}$, the islands collide. The transition could also be seen from the nonlinear evolution of δB_r (Figure 14). With $\upsilon = 3\times10^{-5}$, the DTM experience an abrupt growth at the nonlinear stage (similar to the low shear flow cases), which is an evidence of the occurrence of mode-locking. With lower viscosities, no mode locking occurs. The energy spectrums at $t = 6633 t_A$ (a) $\upsilon = 3\times10^{-6}$ and (b) $\upsilon = 3\times10^{-5}$ are shown in Figure 15. For the low viscosity case, the islands collide, and the KH-like instability becomes dominant at the nonlinear stage. High-m modes gain much energy, and the energy spectrum becomes broad. Magnetic surfaces are destroyed, and the magnetic field becomes stochastic in that region. For the high viscosity case, the two tearing modes are locked with each other, and then experience explosive growth.

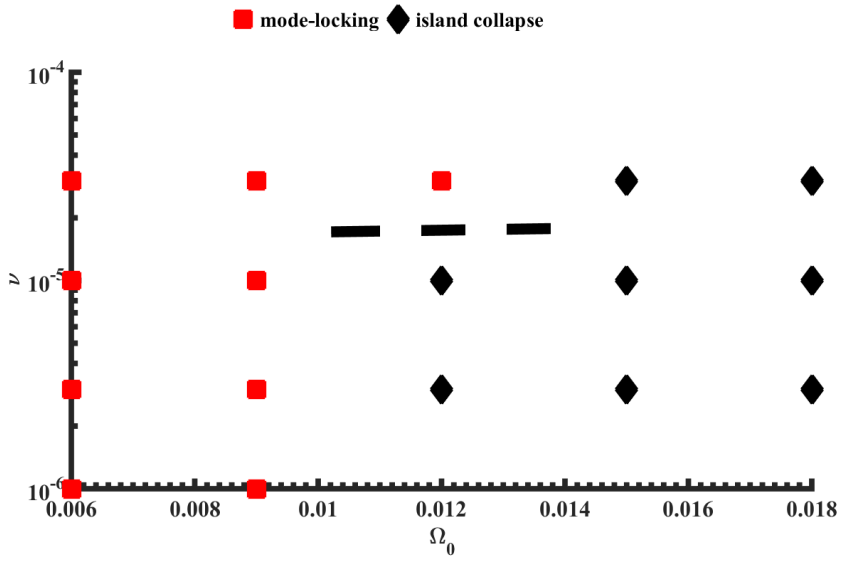

Figure 13 The nonlinear behaviors of the DTM with different Ω_0 and υ.

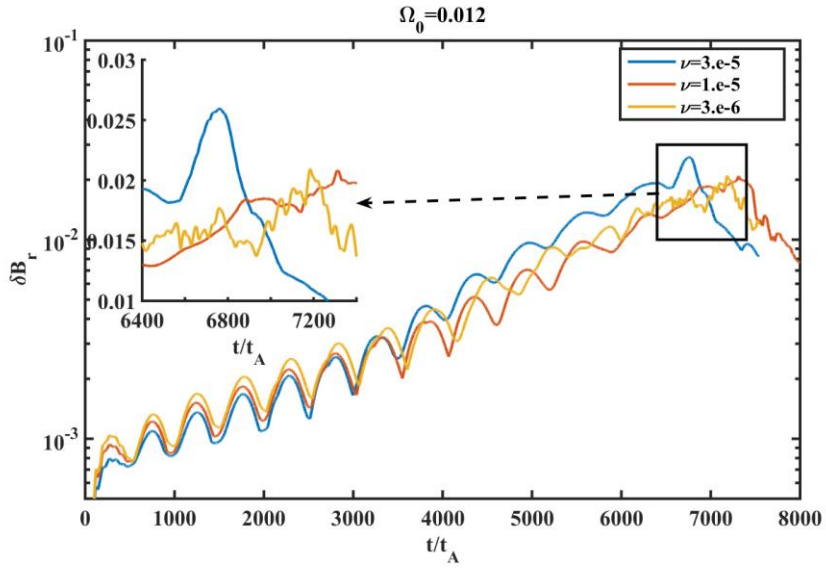

Figure 14 Evolutions of δB_r with different viscosities.

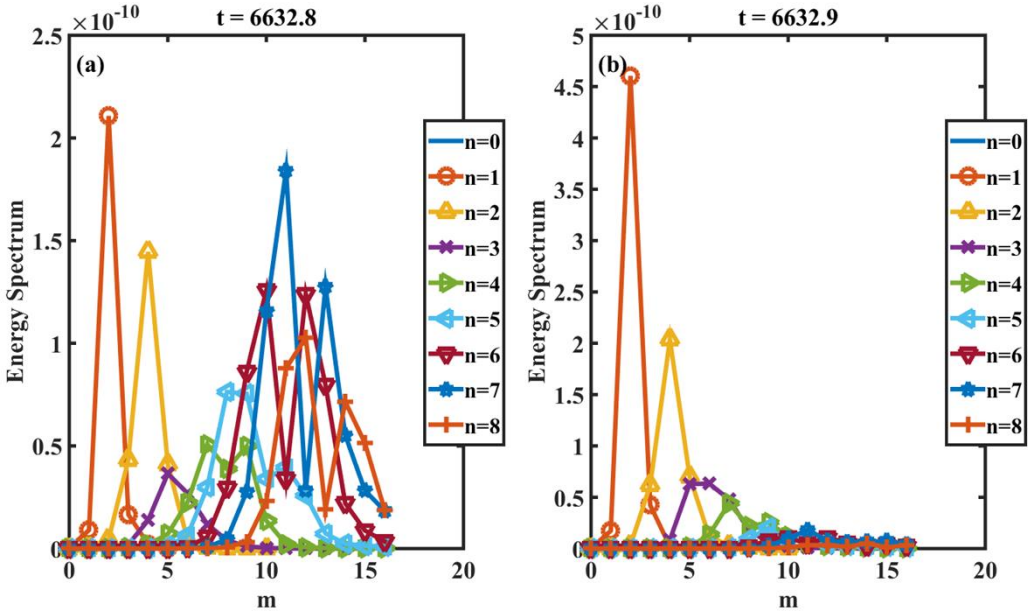

Figure 15 Energy spectra at t=6633t_A (a) $\upsilon = 3\times10^{-6}$ and (b) $\upsilon = 3\times10^{-5}$.

IV. Discussion and conclusion

A series of numerical studies of the influence of shear flows on the dynamic evolutions of the DTM is presented. It is found that weak shear flows can decouple the two tearing modes on the resonant surfaces. As a result, the linear growth rate of the DTM can be substantially reduced. However, it should be noted that the DTM is not fully suppressed, and the amplitude of the DTM slowly grows up. When the DTM's amplitude exceeds the critical value, the two tearing modes can overcome the weak shear flow and become locked. After that, the behavior of the DTM with weak shear flows becomes almost the same as that without shear flows. Although it can decrease the linear growth rate of the DTM, the weak shear flow has almost no influence on the amplitude and the time scale of the pressure crash. It indicates that the shear flow cannot prevent the violent pressure crash.

It is also found that a strong shear flow can even increase the linear growth rate for a reversed magnetic shear system. When the shear flow is stronger than a critical value, the growth rate is even larger than that without shear flows. A KH-like instability can be excited by the strong shear flow, which can lead to a broad energy

spectrum, cause the overlap of the magnetic islands, and then form a vast stochastic magnetic field region. The latter is also destructive for the plasma confinement. As a result, it should be careful to use a shear flow to suppress the DTM in Tokamaks.

Besides, the influence of the viscosity on the nonlinear evolution of DTM is also investigated. It is found that the plasma viscosity becomes important when the shear flow is around a certain value. Around this value, the magnetic islands can be locked at the nonlinear stage with a sufficiently high viscosity; however, the magnetic field becomes stochastic in a broad region due to the islands collide with each other with a low viscosity.

Acknowledgment

This work is supported by the National Natural Science Foundation of China under Grant No. 11775188 and 11835010, the Special Project on High-performance Computing under the National Key R&D Program of China No. 2016YFB0200603, Fundamental Research Fund for Chinese Central Universities.

Reference

[1] F.M. Levinton, M.C. Zarnstorff, S.H. Batha, M. Bell, R.E. Bell, R.V. Budny, C. Bush, Z. Chang, E. Fredrickson, A. Janos, J. Manickam, A. Ramsey, S.A. Sabbagh, G.L. Schmidt, E.J. Synakowski, G. Taylor, Improved Confinement with Reversed Magnetic Shear in TFTR, Physical Review Letters, 75 (1995) 4417-4420.

[2] T. Fujita, S. Ide, H. Shirai, M. Kikuchi, O. Naito, Y. Koide, S. Takeji, H. Kubo, S. Ishida, Internal Transport Barrier for Electrons in JT-60U Reversed Shear Discharges, Physical Review Letters, 78 (1997) 2377-2380.

[3] O. Gruber, R. Wolf, R. Dux, S. Guenter, P.J.M. Carthy, K. Lackner, M. Maraschek, H. Meister, G. Pereverzev, W. Treutterer, t.A.U. Team, Internal transport barrier discharges on ASDEX upgrade: progress towards steady state, Plasma Physics and Controlled Fusion, 42 (2000) A117-A126.

[4] J.W. Connor, T. Fukuda, X. Garbet, C. Gormezano, V. Mukhovatov, M. Wakatani, t.I.T.B.D. Group, t.I.T.G.o. Transport, I.B. Physics, A review of internal transport barrier physics for steady-state operation of tokamaks, Nuclear Fusion, 44 (2004) R1-R49.

[5] Y.X. Wan, J.G. Li, Y. Liu, X.L. Wang, C. Vincent, C.G. Chen, X.R. Duan, P. Fu, X. Gao, K.M. Feng, S.I. Liu, Y.T. Song, P.D. Weng, B.N. Wan, F.R. Wan, H.Y. Wang, S.T. Wu, M.Y. Ye, Q.W. Yang, G.Y. Zheng, G. Zhuang, Q. Li, C. team, Overview of the present progress and activities on the CFETR,

Nuclear Fusion, 57 (2017) 102009.
[6] A.C.C. Sips, f.t.S.S. Operation, t.T.P.t.g. Activity, Advanced scenarios for ITER Plasma Physics and Controlled Fusion, 47 (2005) A19-A40.
[7] Z. Chang, W. Park, E.D. Fredrickson, S.H. Batha, M.G. Bell, R. Bell, R.V. Budny, C.E. Bush, A. Janos, F.M. Levinton, K.M. McGuire, H. Park, S.A. Sabbagh, G.L. Schmidt, S.D. Scott, E.J. Synakowski, H. Takahashi, G. Taylor, M.C. Zarnstorff, Off-Axis Sawteeth and Double-Tearing Reconnection in Reversed Magnetic Shear Plasmas in TFTR, Physical Review Letters, 77 (1996) 3553-3556.
[8] S. Günter, S. Schade, M. Maraschek, S.D. Pinches, E. Strumberger, R. Wolf, Q. Yu, A.U. Team, MHD phenomena in reversed shear discharges on ASDEX Upgrade, Nuclear Fusion, 40 (2000) 1541.
[9] M.R. de Baar, G.M.D. Hogeweij, N.J. Lopes Cardozo, A.A.M. Oomens, F.C. Schüller, Electron Thermal Transport Barrier and Magnetohydrodynamic Activity Observed in Tokamak Plasmas with Negative Central Shear, Physical Review Letters, 78 (1997) 4573-4576.
[10] W. Guo, J. Ma, Q. Yu, Numerical study on nonlinear growth of m/n = 3/1 double tearing mode in high Lundquist number regime, Plasma Physics and Controlled Fusion, 61 (2019) 075011.
[11] T. Liu, J.F. Yang, G.Z. Hao, Y.Q. Liu, Z.X. Wang, S. Zheng, A.K. Wang, H.D. He, Multiple MHD instabilities in high- β N toroidal plasmas with reversed magnetic shear, Plasma Physics and Controlled Fusion, 59 (2017) 065009.
[12] J. Ma, W. Guo, Z. Yu, Q. Yu, Effect of plasmoids on nonlinear evolution of double tearing modes, Nuclear Fusion, 57 (2017) 126004.
[13] A. Bierwage, M. Toma, K. Shinohara, MHD and resonant instabilities in JT-60SA during current ramp-up with off-axis N-NB injection, Plasma Physics and Controlled Fusion, 59 (2017) 125008.
[14] J. Wang, Z.X. Wang, L. Wei, Y. Liu, Control of neo-classical double tearing modes by differential poloidal rotation in reversed magnetic shear tokamak plasmas, Nuclear Fusion, 57 (2017) 046007.
[15] T. Akramov, H. Baty, Non-linear growth of double tearing mode: Explosive reconnection, plasmoid formation, and particle acceleration, Physics of Plasmas, 24 (2017) 082116.
[16] Z.-X. Wang, L. Wei, F. Yu, Nonlinear evolution of neo-classical tearing modes in reversed magnetic shear tokamak plasmas, Nuclear Fusion, 55 (2015) 043005.
[17] G. Sun, C. Dong, L. Duan, Effects of electron cyclotron current drive on the evolution of double tearing mode, Physics of Plasmas, 22 (2015) 092509.
[18] W. Lai, W. Zheng-Xiong, Nonlinear evolution of double tearing modes in tokamak plasmas via multiple helicity simulation, Nuclear Fusion, 54 (2014) 043015.
[19] A. Mao, J. Li, J. Liu, Y. Kishimoto, Zonal flow dynamics in the double tearing mode with antisymmetric shear flows, Physics of Plasmas, 21 (2014) 052304.
[20] P.L. Pritchett, Y.C. Lee, J.F. Drake, Linear analysis of the double-tearing mode, The Physics of Fluids, 23 (1980) 1368-1374.
[21] B. Carreras, H.R. Hicks, B.V. Waddell, Tearing-mode activity for hollow current profiles, Nuclear Fusion, 19 (1979) 583.
[22] Q. Yu, S. Günter, Numerical modelling of neoclassical double tearing modes, Nuclear Fusion, 39 (1999) 487.
[23] A. Mao, J. Li, Y. Kishimoto, J. Liu, Eigenmode characteristics of the double tearing mode in the

presence of shear flows, Physics of Plasmas, 20 (2013) 022114.
[24] M. Janvier, Y. Kishimoto, J.Q. Li, Structure-Driven Nonlinear Instability as the Origin of the Explosive Reconnection Dynamics in Resistive Double Tearing Modes, Physical Review Letters, 107 (2011) 195001.
[25] Z.X. Wang, X.G. Wang, J.Q. Dong, Y.A. Lei, Y.X. Long, Z.Z. Mou, W.X. Qu, Fast Resistive Reconnection Regime in the Nonlinear Evolution of Double Tearing Modes, Physical Review Letters, 99 (2007) 185004.
[26] Y. Ishii, A.I. Smolyakov, M. Takechi, Plasma rotation effects on magnetic island formation and the trigger of disruptions in reversed shear plasma, Nuclear Fusion, 49 (2009) 085006.
[27] L. Wang, W.B. Lin, X.Q. Wang, Effects of resonant magnetic perturbation on the triggering and the evolution of double-tearing mode, EPL (Europhysics Letters), 121 (2018) 45001.
[28] R.B. Zhang, X.Q. Lu, Q.H. Huang, J.Q. Dong, X.Y. Gong, Effect of toroidal plasma rotation on double tearing modes in cylindrical geometry, Physics of Plasmas, 23 (2016) 122509.
[29] X.Q. Wang, X.G. Wang, W. Xu, Z.X. Wang, Interlocking and nonlinear saturation of double tearing modes in differentially rotating plasmas, Physics of Plasmas, 18 (2011) 012102.
[30] Z.-X. Wang, L. Wei, X. Wang, Y. Liu, Self-suppression of double tearing modes via Alfvén resonance in rotating tokamak plasmas, Physics of Plasmas, 18 (2011) 050701.
[31] W. Zhang, Z.W. Ma, S. Wang, Hall effect on tearing mode instabilities in tokamak, Physics of Plasmas, 24 (2017) 102510.
[32] T. Liu, Z.X. Wang, J.L. Wang, L. Wei, Suppression of explosive bursts triggered by neo-classical tearing mode in reversed magnetic shear tokamak plasmas via ECCD, Nuclear Fusion, 58 (2018) 076026.
[33] E.J. Strait, L.L. Lao, M.E. Mauel, B.W. Rice, T.S. Taylor, K.H. Burrell, M.S. Chu, E.A. Lazarus, T.H. Osborne, S.J. Thompson, A.D. Turnbull, Enhanced Confinement and Stability in DIII-D Discharges with Reversed Magnetic Shear, Physical Review Letters, 75 (1995) 4421-4424.
[34] B.W. Rice, K.H. Burrell, L.L. Lao, G. Navratil, B.W. Stallard, E.J. Strait, T.S. Taylor, M.E. Austin, T.A. Casper, M.S. Chu, C.B. Forest, P. Gohil, R.J. Groebner, W.W. Heidbrink, A.W. Hyatt, H. Ikezi, R.J.L. Haye, E.A. Lazarus, Y.R. Lin-Liu, M.E. Mauel, W.H. Meyer, C.L. Rettig, D.P. Schissel, H.E.S. John, P.L. Taylor, A.D. Turnbull, t.D.D. Team, Demonstration of high-performance negative central magnetic shear discharges in the DIII-D tokamak, Physics of Plasmas, 3 (1996) 1983-1991.
[35] J.E. Menard, R.E. Bell, E.D. Fredrickson, D.A. Gates, S.M. Kaye, B.P. LeBlanc, R. Maingi, S.S. Medley, W. Park, S.A. Sabbagh, A. Sontag, D. Stutman, K. Tritz, W. Zhu, t.N.R. Team, Internal kink mode dynamics in high-β NSTX plasmas, Nuclear Fusion, 45 (2005) 539-556.
[36] A. Bierwage, Q. Yu, S. Günter, Large-mode-number magnetohydrodynamic instability driven by sheared flows in a tokamak plasma with reversed central shear, Physics of Plasmas, 14 (2007) 010704.
[37] A. Mao, J. Li, J. Liu, Y. Kishimoto, Nonlinear evolution of the Kelvin-Helmholtz instability in the double current sheet configuration, Physics of Plasmas, 23 (2016) 032117.
[38] H.W. Zhang, J. Zhu, Z.W. Ma, G.Y. Kan, X. Wang, W. Zhang, Acceleration of three-dimensional Tokamak magnetohydrodynamical code with graphics processing unit and OpenACC heterogeneous parallel programming, International Journal of Computational Fluid Dynamics, 33 (2019) 393-406.
[39] S. Wang, Z. Ma, Influence of toroidal rotation on resistive tearing modes in tokamaks, Physics of Plasmas, 22 (2015) 122504.

[40] J. DeLucia, S.C. Jardin, A.M.M. Todd, An iterative metric method for solving the inverse tokamak equilibrium problem, Journal of Computational Physics, 37 (1980) 183-204.
[41] W. Zhang, Z.W. Ma, J. Zhu, H.W. Zhang, Core-crash sawtooth associated with m/n=2/1 double tearing mode in Tokamak, Plasma Physics and Controlled Fusion, (2019).